



# Experimental Study on Damage Morphology and Critical State of Three-Hinge Precast Arch Culvert through Shaking Table Tests

Yasuo Sawamura<sup>1\*</sup>, Hiroyuki Ishihara<sup>2†</sup>,  
Kiyoshi Kishida<sup>3‡</sup> and Makoto Kimura<sup>4§</sup>

<sup>1,4</sup> *Kyoto University, Department of Civil and Earth Resources Engineering, Kyoto, Japan.*

<sup>2</sup> *Kajima Corporation, Hokkaido Branch, Sapporo, Japan*

<sup>3</sup> *Kyoto University, Department of Urban Management, Kyoto, Japan.*

*sawamura.yasuo.6c@kyoto-u.ac.jp, ishihhir@kajima.com,*

*kiyoshi.kishida.3r@kyoto-u.ac.jp, kimura.makoto.8r@kyoto-u.ac.jp*

## Abstract

The three-hinge precast arch culvert is a new type of culvert which consists of two segmental precast units and three hinge points in the body. Since the culvert is outside the range of conventional culverts, which do not consider the seismic behavior in the design, the evaluation of the seismic performance is an important issue. In this study, large-scale shaking table tests were conducted to clarify the seismic behavior and damage morphology of the culvert using a strong earthquake response simulator. From the experimental results, it was confirmed that the hinges did not break before the arch elements reached the ultimate state.

*Keywords:* Precast arch culvert, Damage morphology, Critical state, Damage progression

## 1 Introduction

The three-hinge precast arch culvert is a new type of culvert to save on labor at construction sites, to shorten work periods and to heighten quality control. The culvert consists of two arch members and three hinges in the body. Figure 1 shows the structure of the culvert. The shape is determined to minimize the tensile forces in the arch structure, thus creating an axially loaded structure. The hinge points are at the crown and both feet of the arch. The two arch members are set to incline toward each

\* Created the first stable version of this document

† Created the first draft of this document

‡ Masterminded the this experiment

§ Masterminded the this research work

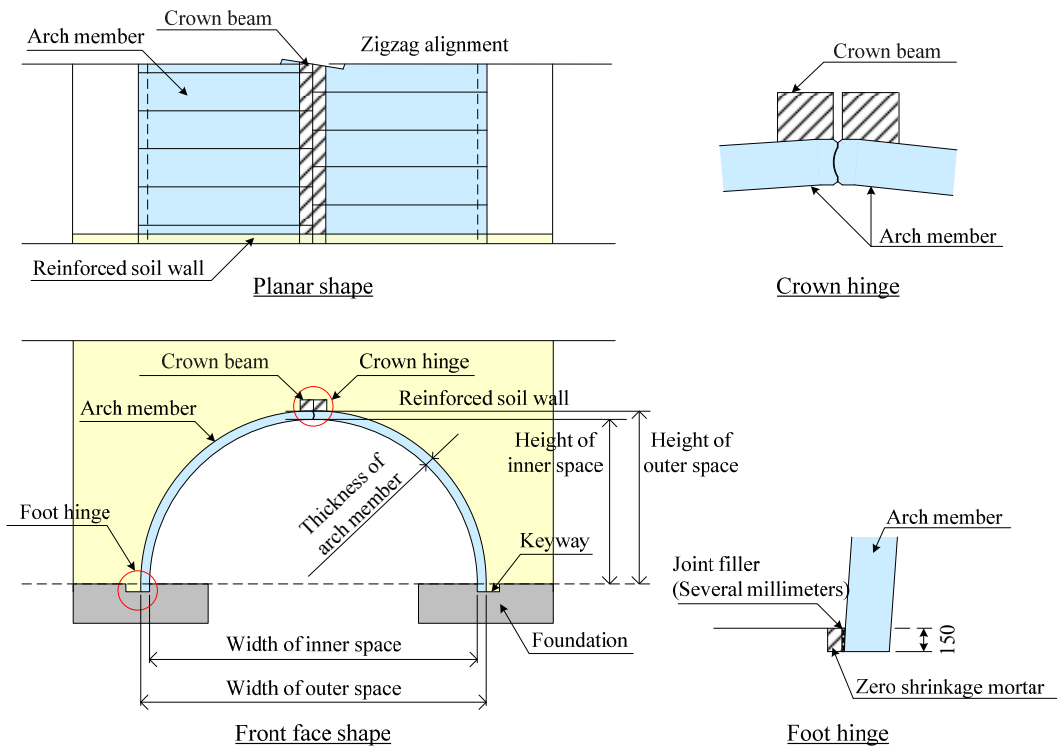


**Figure 1:** Structure of three-hinge precast arch culvert

other to form the crown hinge, and the crown beam is cast in situ to support the arches against longitudinal loads. On the other hand, at each foot hinge, the arch member is supported by an independent concrete strip foundation or a concrete slab. The arch members are placed in simple keyways with a joint filler which appends the hinge function at each foot. A detailed explanation of the design of the culvert has been given in a previous study (Hutchinson, 2004).

As to the design of culverts in Japan, conventional culverts have been built over the past several years by applying methods which do not consider seismic response. This is because such culverts have not suffered terrible damage in past earthquakes. However, the three-hinge precast arch culvert has hinge functions in the main body, and thus, is outside the range of conventional culverts and based on different design concepts. Furthermore, earthquake damage to several three-hinge precast arch culverts was reported after the 2011 Great East Japan Earthquake; hence, it is necessary to investigate the dynamic behavior during strong earthquake motion and the critical state of the culverts.

Regarding the seismic performance of the three-hinge precast arch culvert, some experiments in the 1G gravitational field (Toyota and Takagai, 1999; Toyota and Itoh, 2000) and numerical analyses (Byrne et al. 1996; Wood and Jenkins 2000) have been conducted. However, the damage morphology and the critical state of the culvert have not been clarified. In this study, shaking table tests using a strong earthquake response simulator were conducted to clarify the seismic behavior and the damage morphology of the three-hinge precast arch culvert.

## 2 Experimental condition

Experiments were conducted using the strong earthquake response simulator located at the Disaster Prevention Research Institute at Kyoto University. Figure 2 shows the set-up of the culvert model and the arrangement of the sensors. A soil chamber, about 3.5 m long, 2.0 m deep and 1.0 m wide, was used. Since the lower part of the side wall and the bottom of the soil chamber are connected by a hinge, the side wall serves as a movable wall. Therefore, the soil chamber is a structure which permits simple shear deformation of the culvert and the model ground.

The culvert model was made from reinforced concrete. Table 1 shows the material constants of the model. Kagawa (1978) reported the similarity rule for model tests in the 1G gravitational field. If the similarity rule is applied, it is necessary to reduce the elastic coefficient of the culvert according to the model scale. However, it is difficult to control the elastic coefficient of concrete, and the plastic behavior does not satisfy the rule. Therefore, the 1/5 scale culvert model, whose material parameters for concrete and the reinforcing bar are not reduced, was used in these experiments. Figures 3 and 4 show a drawing of the bar arrangement and photos of the structure of the experimental model, respectively.

Both the foundation ground and the filling were made from Edosaki sand. Table 2 shows the material properties of Edosaki sand. The degree of compaction of Edosaki sand was set to 92%, which is the construction standard for backfill soil in a precast arch culvert. The sand was compacted with the prescribed water

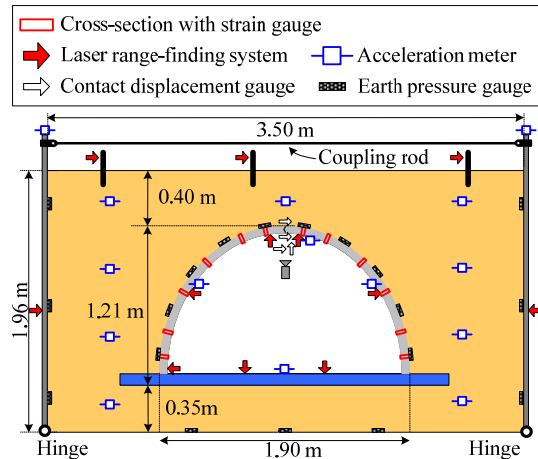


**Figure 2:** Set-up of the culvert model and the arrangement of sensors

**Table 1:** Material constants of culvert model

Property		Culvert
Concrete	Compressive strength $f_c$ [N/mm <sup>2</sup> ]	47.4
	Young's modulus $E_c$ [kN/mm <sup>2</sup> ]	32.4
	Poisson's ratio $\nu_c$	0.18
Reinforced steel	Yield strength $f_y$ [N/mm <sup>2</sup> ]	547.5
	Young's modulus $E_s$ [kN/mm <sup>2</sup> ]	190.2
	Yield strain $\epsilon_y$ [ $\mu$ ]	3000

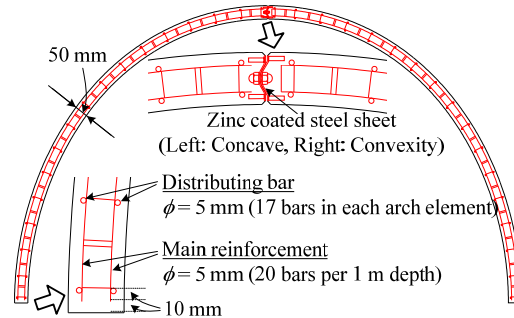


**Figure 3:** Bar arrangement drawing

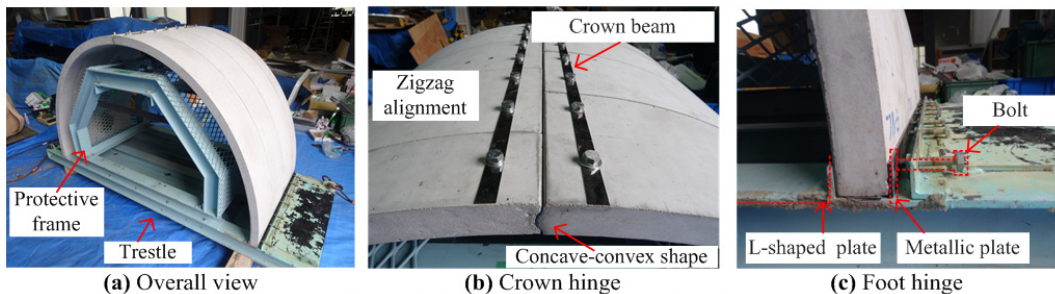


**Figure 4:** Structure of experimental model

**Table 2:** Properties of Edosaki sand

Property	Edosaki sand
Specific gravity of soil particle $G_s$	2.73
Particle size distribution $D_{50}$ [mm]	0.18
Internal friction angle $\phi$ [Deg]	38.3
Cohesion $c$ [kPa]	14.0
Optimum moisture content $w_{opt}$ [%]	20.8
Maximum dry density $\rho_{dmax}$ [g/cm <sup>3</sup> ]	1.64

**Table 3:** Input wave procedure

Step	Type of vibration	Maximum acceleration [m/s <sup>2</sup> ]	Maximum shear strain [%]
1	L1 earthquake	1.46	0.05
2	L2 earthquake	7.57	2.11
3	1 Hz tapered sine wave	6.05	2.07
4	1 Hz tapered sine wave	9.76	7.64

content ( $w = 20.0\%$ ) in 39 layers for every 50 mm.

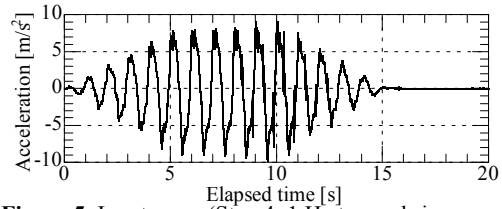
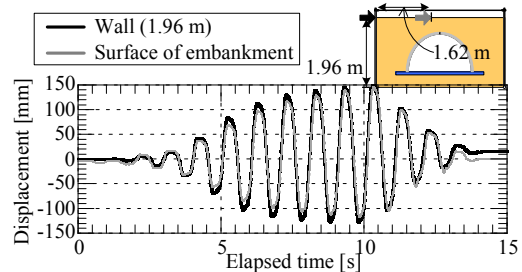
In this study, four types of seismic wave were input. Table 3 shows the input wave procedure. Level 1 and Level 2 earthquake motions (Japan Road Association, 2012), which are often used to design of bridges in Japan, were input in Step 1 and Step 2. However, the culvert model used in these experiments only reduced the scale; the responses against these earthquakes do not show the seismic stability directory. Afterwards, in Step 3 and Step 4, 1 Hz tapered sine waves were input to investigate the damage morphology of the culvert under huge seismic conditions. Figure 5 shows the input seismic motion at Step 4. In this paper, the results of Step 4 are explained. The sampling frequency was 1000 Hz and the total measurement time was 40 seconds.

### 3 Experimental results

#### 3.1 Behavior of precast arch culvert for huge earthquake (Step 4)

Figure 6 shows the time history of the horizontal displacement of the wall (at the height of ground level) and the ground surface at the center of the embankment. The displacement means the relative displacement to the shaking table and the rightward displacement is defined as positive. The displacement of the wall is slightly larger than that of the ground surface. The rightward displacement became maximum at  $t = 10.318$  s, and the maximum displacement at the wall was 149.69 mm and at the surface of the ground was 145.65 mm, respectively. The shear strains, which are calculated by dividing the maximum displacements by the height of ground surface (1.96 m), are 7.64% and 7.43%, respectively. Hamada and Ohmachi (1996) reported that the amount of shear strain not accompanied by liquefaction was 1% in the 1995 Great Hanshin-Awaji Earthquake. In these experiments, therefore, it can be said that very huge shear strain occurred and that the model ground including the culvert greatly deformed.

The dynamic behavior of the three-hinge precast arch culvert is annualized using story drift  $\alpha$  and rigid rotation angle  $\beta$ . As shown in Figure 7, story drift  $\alpha$  is defined as the displacement component which causes a simple shear deformation, while rigid rotation angle  $\beta$  is defined as the displacement


**Figure 5:** Input wave (Step 4 : 1 Hz tapered sine wave)

**Figure 6:** Time history of horizontal displacement

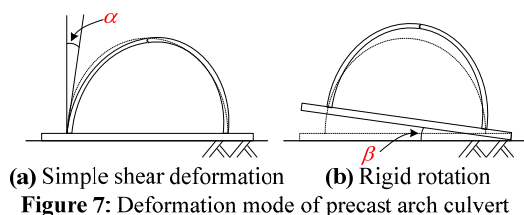


Figure 7: Deformation mode of precast arch culvert

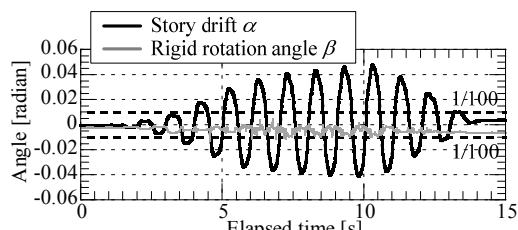


Figure 8: Time history of story drift  $\alpha$  and rigid rotation angle  $\beta$

component which revolves like a rigid body without transformation. Figure 8 shows the time history of story drift  $\alpha$  and rigid rotation angle  $\beta$ . Although a correlation is seen between these values, rigid rotation angle  $\beta$  is imperceptible compared to story drift  $\alpha$ . Hence, it means that the simple shear deformation dominates in the dynamic behavior of the three-hinge precast arch culvert. Story drift  $\alpha$  and the horizontal displacements of the wall and the embankment become maximum at the same time. Thus, it can be said that the deformation and the cross-sectional force of the culvert are dominated by the oscillatory displacement of the surrounding ground.

The horizontal displacements of the culvert and the surrounding ground at  $t = 10.318$  s are shown in Figure 9. Since the displacements of the crown and both shoulders of the culvert are smaller than that of the ground, it is thought that the culvert has experienced rightward force from the left-hand side banking. Focusing attention on the displacement at both shoulders, the displacement at the left shoulder is 20 mm larger than that at the right shoulder, and thus, the culvert deformed largely with the mode wherein the left arch element displaced inside of the arch.

Figure 10 shows the distribution of earth pressure acting on the culvert at  $t = 10.318$  s. The dashed line means the initial earth pressure. The earth pressure acting on the left shoulder increases from the initial state, while the earth pressure acting on the right shoulder decreases to the value of zero. Therefore, it is thought that the right shoulder part of the culvert and the ground may be separated during a large earthquake. Figure 11 shows the distribution of strain generated in the reinforcing bar. The tensile strain is defined as positive. When the culvert and the ground deform in a rightward direction, the culvert experiences rightward force from the ground; and hence, large tensile strain occurs inside of the left arch member and outside of the right arch member. From these results, it is clear that the seismic response of a culvert can be explained from the relative displacement between

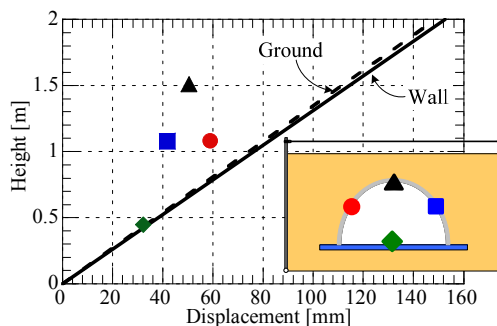


Figure 9: Horizontal displacement of culvert and ground at  $t = 10.318$  s

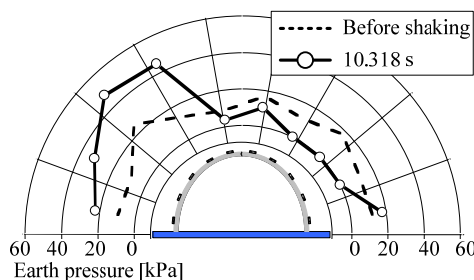


Figure 10: Distribution of earth pressure at  $t = 10.318$  s

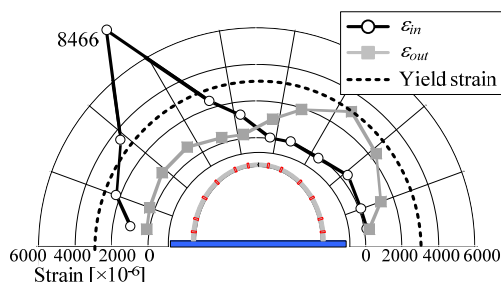


Figure 11: Distribution of steel strain at  $t = 10.318$  s

the culvert and the ground, as shown in Figure 9. Therefore, the dynamic behavior of a culvert is governed by the shear deformation of the surrounding soil, and it is probable that seismic deformation methods, like the “responded displacement method” and the “seismic coefficient method”, are applicable to the aseismic design of three-hinge precast arch culverts.

Figure 12 shows the time history of the strain generated in the reinforcing bar at the left shoulder (L-4). The strain of the inside reinforcing bar gradually increased from the initial state and reached the yield strain at around 6 seconds. The plastic strain accumulates with the vibration, and finally the strain reaches more than 8000  $\mu$  which is 2.8 times the yield strain. Figure 13 shows the relation between the horizontal force acting on the culvert and the horizontal displacement of the left arch member. The horizontal force is calculated from the measured earth pressure. From Figure 13, it can be seen that the gradient of the hysteresis curve gradually decreases. This is because the whole rigidity of the culvert decrease brings about the development of failure.

Figure 14 shows the time history of the rotation angle of the crown hinge. The rotation angle accumulates as the whole arch transforms convexly. The residual value after the earthquake is 0.043 radian (2.45 degrees). Although it is feared that the crown hinge will drop out during an earthquake, it is confirmed that the possibility for the whole culvert to collapse due to the omission of a hinge part is low even when the shear strain of the ground is more than 7% and the strain of the reinforcing bar reaches 2.8 times the yield strain.

Figure 15 shows the points and the order of the reinforcing bars which reach the yield strain. In this figure, the time when the strain of the reinforcing bar reached the yield strain (3000  $\mu$ ) for the first time at each measurement location is arranged. From Figure 15, it can be seen that the damage proceeds from the inside reinforcing bar. This is because the arch members are likely to deform inwardly during an earthquake. It is advisable to view this damage process from the perspective of

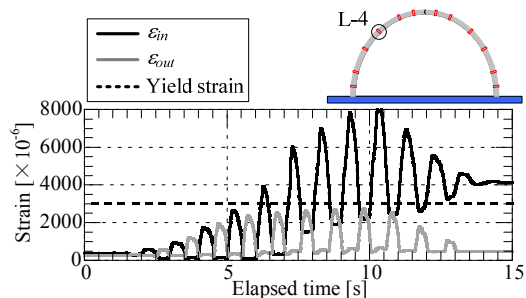


Figure 12: Time history of steel strain at L-4

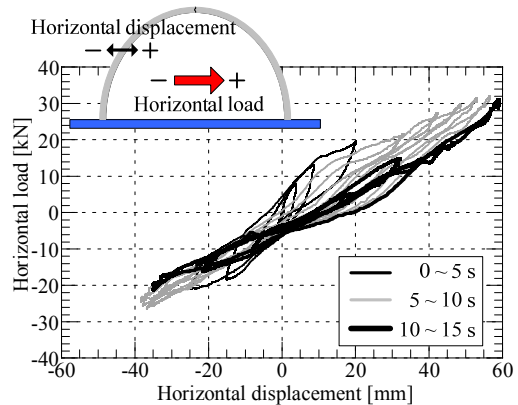


Figure 13: Relation between horizontal load and displacement

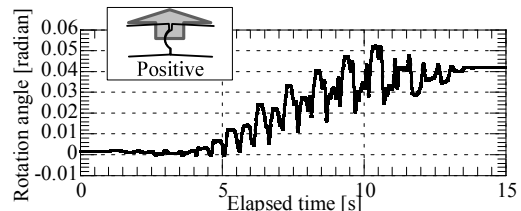


Figure 14: Time history of rotation angle of crown hinge

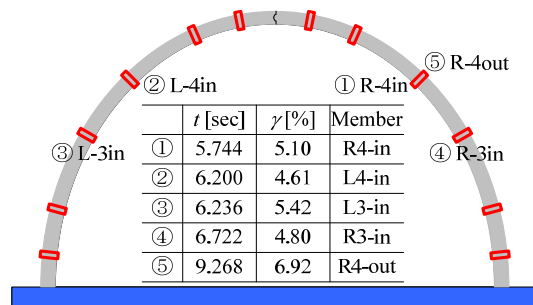
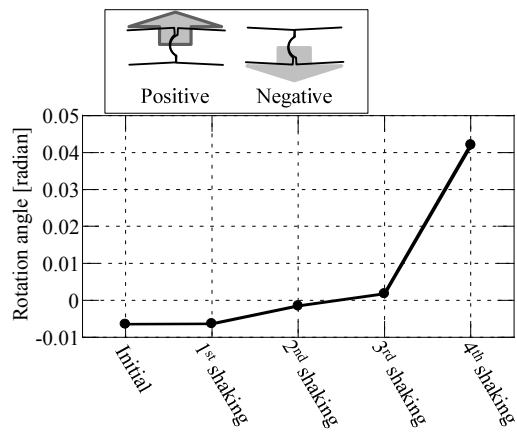
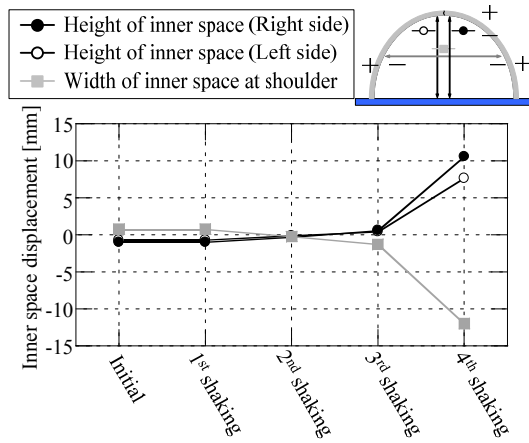
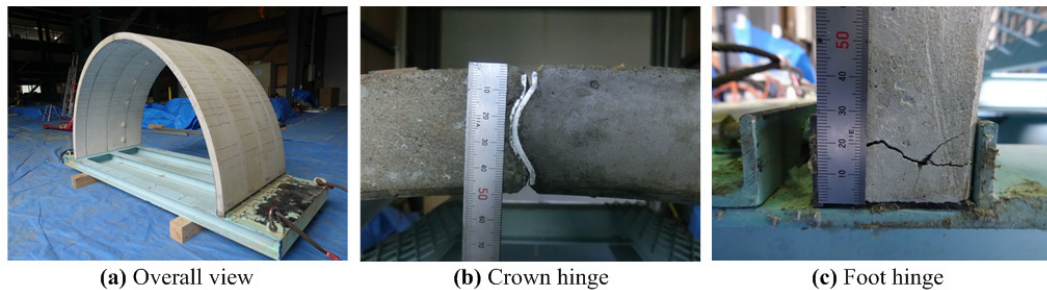


Figure 15: Points and order of yield steel



**Figure 16:** Transition of height and width of inner space **Figure 17:** Transition of rotation angle of crown hinge



**Figure 18:** Damage of culvert after experiment

maintenance. This is because visual confirmation is possible, although it is difficult to confirm the damage to culverts in comparison to bridges.

### 3.2 Transition of inner space and damage conditions of culvert

Figures 16 and 17 show the transition of the inner displacement of the culvert and the rotation angle of the crown hinge, respectively. From these figures, it is confirmed that the width of the inner space narrows, the height of the inner space grows wider and the rotation angle of the crown hinge accumulates toward the ground side. These tendencies are conspicuous in Step 4 during which large damage is generated. Therefore, with in situ construction, it is thought that damage to the culvert can be estimated by measuring the inner space displacement after an earthquake.

Figure 18 shows the damage conditions of the culvert after the experiments. Equally-spaced cracks are generated at the location of the hoop tie both inside and outside of the arch member. The damage to the inside of the arch member was heavier than that to the outside, namely, the crack widths at the inside and outside were 0.2 mm and 0.15 mm, respectively. From the visual confirmation, it was seen that no gaps were generated in the arch member and no cracks were generated around the hinge at the crown hinge. On the other hand, at the foot hinge, a large crack appeared about 15 mm from the bottom. This is because both feet hinges were modeled by bookending using a metal plate with a bolt (shown in Figure 4), and the rotation stiffness in the experiments was larger than that under in situ conditions. However, the rotation stiffness of the foot hinge might be zero after the generation of large cracks. From the results, it was confirmed that the hinge part did not break antecedent to the ultimate behavior of the arch element under such circumstances.

## 4 Conclusion

In this study, large-scale shaking table tests using a strong earthquake response simulator were conducted to clarify the seismic behavior of the three-hinge precast arch culvert. From the results, the following conclusions can be drawn from the results of this study:

1. The seismic response of the culvert can be explained by the relative displacement between the culvert and the ground even when a large earthquake occurs and the shear strain of the ground rises to more than 7%. Therefore, the dynamic behavior of the culvert is governed by the shear deformation of the surrounding soil, and it is probable that seismic deformation methods, like the “responded displacement method” and the “seismic coefficient method”, are applicable to the aseismic design of three-hinge precast arch culverts.
2. Although it is feared that the crown hinge will be drop out during an earthquake, it is confirmed that the possibility for the whole culvert to collapse due to the omission of a hinge part is low even when the shear strain of the ground is more than 7% and the strain of the reinforcing bar reaches 2.8 times the yield strain.
3. Damage to the three-hinge precast arch culvert proceeds from the inside reinforcing bar. It is advisable to view this damage process from the perspective of maintenance. This is because visual confirmation is possible, although it is difficult to confirm the damage to culverts compared to bridges.
4. The residual displacement of the culvert is accumulated unidirectionally. Therefore, it is thought that the damage to culverts can be estimated by measuring the inner space displacement after an earthquake.

## References

- Hutchinson, D. (2004). Application and Design of Segmental Precast Arches. *Geotechnical Engineering for Transportation Projects*: pp. 452-459. (doi:10.1061/40744(154)30)
- Toyota, H., and Takagai, M. (1999). Dynamic Behavior of 3-hinge Arch in Terre Armee Foundation, *Journal of Geotechnical Engineering*, No. 624/III-47, pp. 255-266, 1999. (in Japanese)
- Toyota, H. and Itoh, T. (2000). Effects of Shaking Conditions and Material Properties on Dynamic Behavior of Terre Armee Foundation and 3-Hinge Arch, Proc. of Japan Society of Civil Engineers, No. 666/III-53, pp. 279-289. (in Japanese)
- Byrne, P. M., Anderson, D. L., and Jitno, H. (1996). Seismic analysis of large buried culvert structures. *Transportation Research Record 1541*, Transportation Research Board, Washington, DC, pp. 133-139. (<http://dx.doi.org/10.3141/1541-17>)
- Wood, J. H., and Jenkins, D. A. (2000). Seismic analysis of buried arch structures. *Proc. of 12th World Conf. on Earthquake Engineering*, New Zealand Society for Earthquake Engineering, Wellington, New Zealand.
- Kagawa, T. 1978. On the similitude in model vibration tests of earth-structures, *Proc. of Japan Society of Civil Engineers*, No. 275, pp. 69-77. (in Japanese)
- Japan Road Association. (2012). Design specifications of highway bridges. Part V: Seismic design. (in Japanese)
- Hamada, M. and Ohmachi, T. (1996). Evaluation of Earthquake-induced Displacement and Strain of the Surface Ground in Near-field, *Hanshin-Awaji Dai-shinsai ni kansuru Gakujyutsu-Kouenkai ronbunshyu* pp. 69-80. (in Japanese)